

Optimal Power Flow in Microgrids With Energy Storage

Yoash Levron, Josep M. Guerrero, *Member, IEEE*, and Yuval Beck

Abstract—Energy storage may improve power management in microgrids that include renewable energy sources. The storage devices match energy generation to consumption, facilitating a smooth and robust energy balance within the microgrid. This paper addresses the optimal control of the microgrid’s energy storage devices. Stored energy is controlled to balance power generation of renewable sources to optimize overall power consumption at the microgrid point of common coupling. Recent works emphasize constraints imposed by the storage device itself, such as limited capacity and internal losses. However, these works assume flat, highly simplified network models, which overlook the physical connectivity. This work proposes an optimal power flow solution that considers the entire system: the storage device limits, voltages limits, currents limits, and power limits. The power network may be arbitrarily complex, and the proposed solver obtains a globally optimal solution.

Index Terms—Distributed generation (DG), energy storage, microgrid, optimal power flow (OPF), smart grid.

I. INTRODUCTION

MICROGRIDS have received increasing attention as a means of integrating distributed generation into the electricity grid [1], [2]. Usually described as confined clusters of loads, storage devices, and small generators, these autonomous networks connect as single entities to the public distribution grid, through a point of common coupling (PCC). Fig. 1 illustrates a typical microgrid network. Microgrids comprise a variety of technologies: renewable sources, such as photovoltaic and wind generators are operated alongside traditional high-inertia synchronous generators, batteries and fuel-cells [3]. Thus, energy is generated near the loads, enabling the utilization of small-scale generators that increase reliability, and reduce losses overlong power lines.

The locality of the microgrid network enables an improved management of energy. Generators (and possibly loads) may be controlled by a local energy management system (EMS) to optimize power flow within the network. The objectives of energy management depend on the mode of operation: Islanded, or grid-connected.

Manuscript received July 22, 2012; revised September 19, 2012, November 07, 2012, and December 27, 2012; accepted February 02, 2013. Date of publication February 22, 2013; date of current version July 18, 2013. Paper no. TPWRS-00860-2012.

Y. Levron is with the Department of Electrical Engineering, Technion Institute of Technology, Haifa 32000, Israel (e-mail: yoashlevron@gmail.com).

J. M. Guerrero is with the Institute of Energy Technology, Aalborg University, 9220 Aalborg East, Denmark (e-mail: joz@et.aau.dk).

Y. Beck is with the Electrical Engineering Faculty, Holon Institute of Technology, 58102 Holon, Israel (e-mail: beck@hit.ac.il)

Color versions of one or more of the figures in this paper are available online at <http://ieeexplore.ieee.org>.

Digital Object Identifier 10.1109/TPWRS.2013.2245925

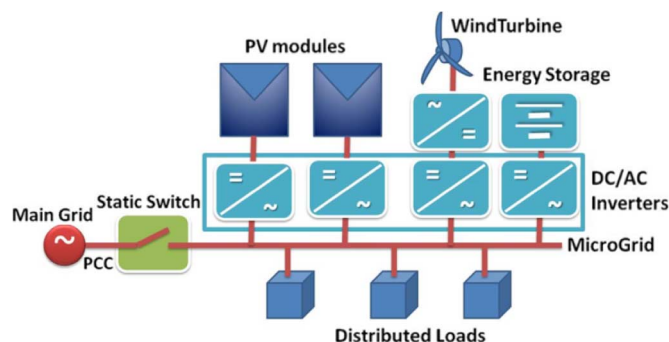


Fig. 1. Typical microgrid.

In islanded mode, the main goal of power management is to stabilize the system, in terms of frequency and voltage. In grid-connected mode, typical objectives are to minimize the price of energy import at the PCC, to improve power factor at the PCC, and to optimize the voltage profile within the microgrid [4], [5]. This work addresses grid-connected networks.

Energy management in microgrids is usually thought of as a three-level hierarchical control system [6]. The first control level, often called “primary” or “autonomous” control, consists of a number of local, autonomous controllers. Each controller governs a power electronics converter and is responsible to interface generators, storage devices, and loads with the microgrid [7]. These controllers are the fastest, as they operate in the millisecond range, employing a droop control in islanded mode [2]. A secondary control level employs a low-bandwidth communication to fix the frequency and amplitude of the microgrid’s units, restoring their nominal values. Finally, the tertiary control level [1], [6] is related to the control of active and reactive power flow. This level of control is related to EMS (see [2]) and to the optimization of the microgrid resources and is the main subject of this work.

The tertiary control-level coordinates power flow within the microgrid and therefore often utilizes an optimal power flow (OPF) solver. Such solvers have been extensively studied by many. Surveys may be found at [8] and [9]. However, classical power flow solutions are not tailored for microgrid analysis, particularly due to the lacking representation of distributed energy sources, storage devices, and pricing methods. Recently, several studies have shown optimal power flow models that highlight the unique aspects of microgrids. These studies can be categorized by focus. A first group studies the allocation and optimal power sharing of distributed generators, most often solar or wind [10], [11]. A second group highlights the economic revenue. Their objective is usually to minimize the overall price of

energy or to maximize the profit from energy generation [6], [12].

A third group examines the optimal dispatch of energy storage devices [13]–[16]. Energy may be stored when renewable power is available or when energy import is inexpensive. This stored energy may be consumed later when demand is high or when renewable power is unavailable. The objective here is to optimize price, efficiency, and stability, considering the constraints imposed by the storage devices, such as limited capacity and internal losses. For example, in studies [13], [14], the storage device operates as a mediator of power generation. Overall power generation is optimized to be as constant as possible, reducing fuel costs, while taking into account the limited storage capacity. The study in [15] employs storage to time-shift the generation of renewables, matching generation to consumption. The study in [16] addresses a wind farm, compensated by a battery energy storage. Their goal is to control the storage device for improving the predictability of power generation.

All of the above studies assume trivial network topologies. None of them inspect storage devices integrated in a general power network. An optimal solution to a generally meshed network with storage devices has not been shown. The reason for this is the tremendous numerical complexity of the problem, which includes both the network domain and the time domain, related with storage. Traditional gradient based solvers (such as Newton-Raphson), while extremely useful in the network domain, are inadequate in the time domain and cannot be applied to the combined network-storage problem (see details in Section III).

To cover this gap, this work introduces a new solution method to this problem: an optimal power flow (OPF) solver that integrates storage devices. The suggested method computes the globally optimal power flow, in both the network and time domains. It considers both the limitations of the storage device and the limitations of the network regarding voltages, currents and powers. The method combines a power flow solver with a dynamic programming recursive search, achieving a numerically efficient solution.

II. NETWORK TOPOLOGY AND POWER FLOW EQUATIONS

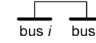

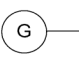

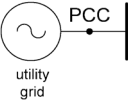
This work utilizes the usual terminology of a power-flow analysis [8]. Buses are denoted with the running index i , where $i = 1 \dots N$. N is the number of buses. Each bus is described by four independent signals:

- $P_i(t)$ —the active power, injected from the bus into the grid (positive for generators, negative for loads);
- $Q_i(t)$ —the reactive power, injected into the grid;
- $V_i(t)$ —the voltage magnitude of the bus;
- $\delta_i(t)$ —the phase angle of the voltage V_i .

Basic units of the microgrid are defined in Table I. It describes single phase units, balanced three-phase units, or unbalanced three-phase units, with per phase representation (“x” denote the phase, A, B, or C and is omitted for balanced three-phase).

The PCC corresponds to the “slack” bus. It is always indexed as bus 1 ($i = 1$) and is described as a $V - \delta$ bus, with $V_1(t) = V_{in}(t)$ as an uncontrollable voltage signal. Loads and renewable

TABLE I
UNITS OF THE MICROGRID

Unit	Symbol	Constraints	model refs
power line		Constraints: $I_{i,j,x}(t) < I_{i,j,max}$	
load		Constraints: $P_{i,x}(t) = -P_{L,ix}(t)$ (fixed) $Q_{i,x}(t) = -Q_{L,ix}(t)$ (fixed) $V_{ix,min} \leq V_{ix}(t) \leq V_{ix,max}$ Free variables: $V_{ix}(t), \delta_{ix}(t)$	
Renewable generator		Constraints: $P_{ix}(t) = +P_{g,ix}(t)$ (fixed) $Q_{ix}(t) = +Q_{g,ix}(t)$ (fixed) $V_{ix,min} \leq V_{ix}(t) \leq V_{ix,max}$ Free variables: $V_{ix}(t), \delta_{ix}(t)$	
storage device		$E_{ix}(t)$ = stored energy or state of charge (SOC). Typical constraints: $V_{ix}(t) = V_{S,i}$ (fixed) $0 \leq E_i(t) \leq E_{i,max}$ $-P_{i,rated} \leq P_i(t) \leq +P_{i,rated}$ State equation (one-phase): $\frac{d}{dt} E_i = f_i(P_i, E_i)$ Free variables: $P_i(t), Q_i(t), \delta_i(t), E_i(t)$	[13]–[15]
point of common coupling (PCC)		The PCC is always indexed as bus 1, $i=1$. Constraints: $\delta_{1,x}(t) = 0$ $V_{1,x}(t) = V_{in,x}$ (fixed) $Q_{1x,min} \leq Q_{1,x}(t) \leq Q_{1x,max}$ $P_{1x,min} \leq P_{1,x}(t) \leq P_{1x,max}$ Free variables: $P_I(t), Q_I(t)$	[8], [10]

generators are uncontrollable and are therefore represented by fixed power signals (power versus time). For a balanced three-phase system, power-flow equations are given in

$$\begin{aligned}
 P_i &= V_i \cdot \sum_{j=1}^N Y_{ij} \cdot V_j \cdot \cos(\delta_i - \delta_j - \theta_{ij}) \\
 Q_i &= V_i \cdot \sum_{j=1}^N Y_{ij} \cdot V_j \cdot \sin(\delta_i - \delta_j - \theta_{ij}) \\
 I_{ij} &= |V_i \cdot e^{i\delta_i} - V_j \cdot e^{i\delta_j}|.
 \end{aligned} \tag{1}$$

These may be found in many classical textbooks, such as [8]. In (1), Y_{ij} and θ_{ij} are the admittances' magnitude and phase, Y_{ii} are the self-admittances, Y_{ij} ($i \neq j$) are the cross admittances, and I_{ij} are the line currents (magnitude).

The system may also be an unbalanced three-phase system. The power flow equations for this case are too complex to be described in the present scope, and are fully detailed in [17]. For a simplified unbalanced system, in which leakage currents are neglected, and the neutral line impedances are taken as zero, the power-flow equations are given by

$$\begin{aligned}
 P_{i,x} &= V_{i,x} \cdot \sum_{j=1}^N Y_{ij,x} \cdot V_{j,x} \cdot \cos(\delta_{i,x} - \delta_{j,x} - \theta_{ij,x}) \\
 Q_{i,x} &= V_{i,x} \cdot \sum_{j=1}^N Y_{ij,x} \cdot V_{j,x} \cdot \sin(\delta_{i,x} - \delta_{j,x} - \theta_{ij,x}) \\
 I_{ij,x} &= |V_{i,x} \cdot e^{i\delta_{i,x}} - V_{j,x} \cdot e^{i\delta_{j,x}}|
 \end{aligned} \tag{2}$$

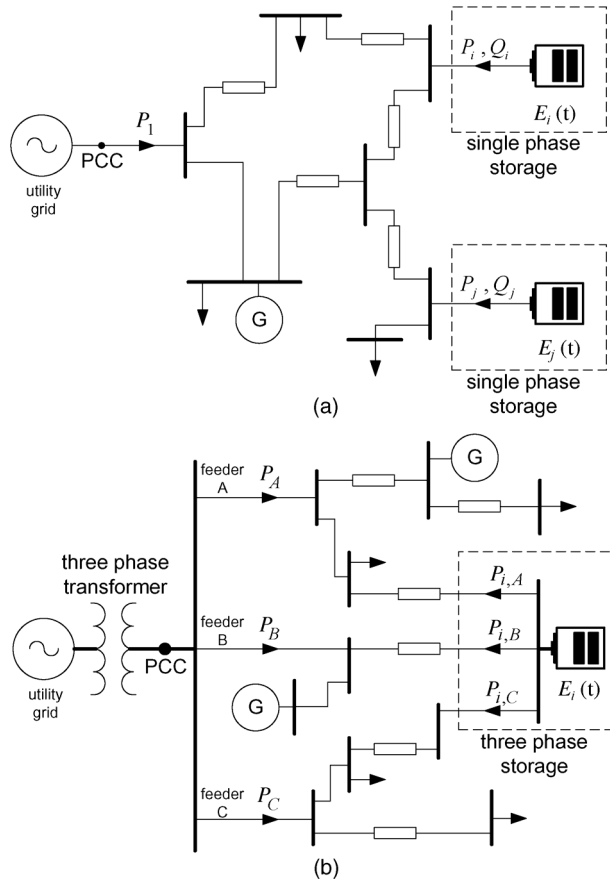


Fig. 2. Notations of one-phase or three-phase networks and storage devices. (a) Single phase system with two storage devices. (b) Three phase system with a three-phase device.

where the subindex “x” represents the phase A, B or C. Section IV explained how these various system representations are integrated in the proposed time-domain solver.

Storage devices are modeled by an inner state variable—the stored energy $E_i(t)$. They are defined by a general state equation $f(\cdot)$, given by the following.

One-phase storage device:

$$\frac{d}{dt}E_i = f_i(P_i, E_i). \quad (3)$$

Three-phase storage device:

$$\frac{d}{dt}E_i = f_i(P_{i,A}, P_{i,B}, P_{i,C}, E_i) \quad (4)$$

where $P_{i,A}, P_{i,B}, P_{i,C}$, are the three phase powers at the PCC [see Fig. 2(b)].

The objective is to minimize the overall cost of energy import from the public grid, determined by incoming power at the PCC. For a single-phase system, the objective is

$$\int_0^T P_1(t) \cdot C(t) dt \rightarrow \min \quad (5)$$

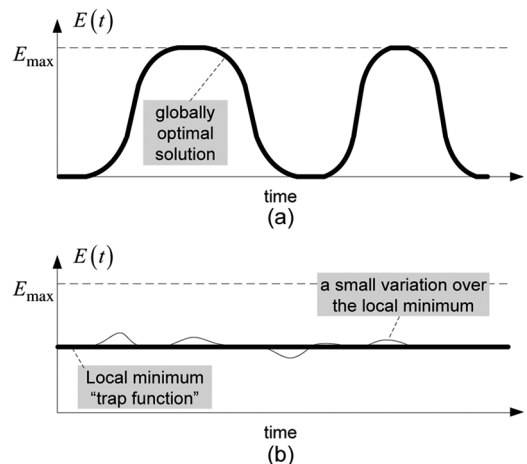


Fig. 3. Global and local solutions in time domain. (a) Global solution. (b) Local solution (bold) with a small variation (thin). The variation is energetically worse than the local solution, due to charge and discharge losses.

where $C(t)$ is a price signal (\$/MW), which is usually a time-dependent function. For an unbalanced three-phase system (Fig. 2), the objective is

$$\int_0^T (P_A(t) + P_B(t) + P_C(t)) \cdot C(t) dt \rightarrow \min \quad (6)$$

An alternative objective for unbalanced three-phase systems may be balancing the power among the three phases:

$$\int_0^T (P_A(t) - P_B(t))^2 + (P_B(t) - P_C(t))^2 dt \rightarrow \min. \quad (7)$$

III. GRADIENT-BASED SOLVERS IN THE TIME DOMAIN

An optimal solution demands the computation of powers (P, Q), voltages (V), currents (I), phase angles (δ), and stored energy (E). All of these quantities are time-dependent. While gradient-based solvers (like Newton-Raphson) have been proven to solve networks efficiently, they are inadequate for storage problems. Here, we explain this claim.

The desired solution is a function of stored energy versus time $E(t)$. To reach a solution, the solver must determine $E(t)$ at every time point, thus each time point is a free variable. Apparently, many time-energy functions are local minima. Consider, for instance, the straight line in Fig. 3(b). Assume a small perturbation over this possible solution. Due to inefficiencies of the storage device, charging and discharging are wasteful, therefore, with respect to the objective, the perturbation is less efficient and is worse than the straight line solution. The straight line is therefore “surrounded” by solutions which are worse and are, in fact, a local minimum.

While this explanation is by no means a mathematical proof, it highlights the numerical difficulties of gradient-based solvers, applied to time-domain problems. If a gradient-based solver reaches a local solution, such as the straight line in Fig. 3(b), it will conclude that it is optimal. However, this local solution

does not resemble the global one and have no desired properties. This local solution is unsuitable and cannot be used in a real power system.

IV. DYNAMIC PROGRAMMING APPROACH

Unlike gradient-based methods, dynamic programming algorithms (see [18]) scan all feasible solutions to locate the global optimum. A direct scan of the entire solution space is numerically impossible, so the optimal solution is designed recursively, combining dynamic allocation in the time domain, with a traditional power flow solver on the network domain.

A. Single Storage Device—One-Dimensional Solution

With a single one-phase storage device, the stored energy function $E_i(t)$ governs the power flow of the network. For a given energy function, the power output of the storage device $P_i(t)$ may be computed using the storage state (3). Assuming that the voltage magnitude of the device is specified, $V_i(t) = V_{S,i}$, the device may be replaced by an auxiliary P - V unit, with known power and voltage values. Recall that loads and renewable generators are specified, so given the storage power output, power flow over the entire network may be computed. This is easily achieved using standard power flow algorithms, such as Gauss–Seidel, or Newton–Raphson. The problem is therefore one-dimensional, with a single controllable state variable $E_i(t)$.

The challenge is to determine the energy function $E_i(t) = E(t)$ that minimize the objective equation (5) and comply with all constraints listed in Table I. To this end, a value function $V(\cdot)$ is defined as

$$V(t, E) = \int_t^T P_1(\tau) \cdot C(\tau) \cdot d\tau \quad (8)$$

with an initial condition $E(t) = E$

The objective equation (5) is equivalent to minimizing $V(0, 0)$, that is, to minimize overall cost over the entire period, starting with an empty storage $E = 0$. Calculations are numeric, over a discrete grid. dt marks the time step, and dE marks the energy step. The optimal solution is computed recursively by the Bellman equation

$$V(t, E) = \min_{E(t+dt)} \{ \Delta V(E, E(t+dt)) + V(t+dt, E(t+dt)) \} \quad (9)$$

The value function $V(t, E)$ is numerically computed by backward recursion. The process starts at the final time $t = T$, where the value function is known: $V(T, E) = 0$. Applying (9), the value function may be computed at $T - dt$, revealing $V(T - dt, E)$ over all the energy values. The process continues until reaching $t = 0$. A backward recursion step is shown at Fig. 4(a).

The differential cost ΔV is defined for every two arbitrary points $\{t, E(t)\}$ and $\{t + dt, E(t + dt)\}$. It represents the cost of transition between the two points. ΔV is computed in the following steps.

Step 1) The first derivative of energy is evaluated by

$$\frac{d}{dt} E \approx \frac{E(t + dt) - E(t)}{dt}. \quad (10)$$

Step 2) Power output of the storage device, $P_i(t)$, is evaluated. The storage state (3) is solved using known values of $E(t)$ and its first derivative $E'(t)$, revealing $P_i(t)$.

Step 3) The storage device is replaced with an auxiliary P - V source, with $P = P_i(t)$, $V = V_{S,i}$. A network power flow analysis is computed using Gauss–Seidel, Newton–Raphson, or any other method.

Step 4) If the power flow solution complies with all network constraints, the differential ΔV is assigned a value according to the power at the PCC, $P_1(t)$. Otherwise, it is assigned a value of infinity

$$\Delta V = \begin{cases} P_1(t) \cdot C(t) \cdot dt, & \text{in constraints} \\ \infty, & \text{otherwise} \end{cases}. \quad (11)$$

Having computed $V(t, E)$ over all times and energies, the optimal energy $E^*(t)$ may be evaluated. This is done by a forward recursion process. Known values of $V(t, E)$ are substituted in the Bellman equation to recover the optimal solution

$$E^*(t) = \arg \min_{E(t)} \{ \Delta V(E^*(t-dt), E(t)) + V(t, E(t)) \} \quad (12)$$

Energy at t and $E^*(t)$ is calculated in relation to a previous energy value $E^*(t - dt)$. The computation process starts at $t = 0$, in which optimal energy is known and equals the starting condition, usually $E^*(0) = 0$. Optimal energy at the next time step $E^{ast}(dt)$ is evaluated by (12). The process continues until the entire optimal energy path has been discovered, up to the final time $t = T$. Knowing the optimal energy path, all powers, voltages, and phase angles may be computed directly.

B. Multiple Storage Devices

Each storage device adds a dimension to the solution space. Thus, a network with two storage devices is a two-dimensional (2-D) problem, with two free variables: $E_i(t)$ and $E_j(t)$. Power flow is now governed by two energy functions instead of one. A 2-D computation is shown in Fig. 4(b).

Multidimensional solutions are essentially equivalent to single dimension solutions. The major difference is that the value function, $V(\cdot)$ is now multidimensional. Consider, as an example, a one-phase network with two storage devices. The value function is now defined as follows:

$$V(t, E_i, E_j) = \int_t^T P_1(\tau) \cdot C(\tau) \cdot d\tau \quad (13)$$

initial condition

$$E_i(t) = E_i, \quad E_j(t) = E_j.$$

It is a function of both $E_i(t)$ and $E_j(t)$. The Bellman equation now involves minimization over both energy variables

$$V(t, E_i, E_j) = \min_{\substack{E_i(t+dt), \\ E_j(t+dt)}} \{ \Delta V(E_i, E_i(t+dt), E_j, E_j(t+dt)) + V(t+dt, E_i(t+dt), E_j(t+dt)) \} \quad (14)$$

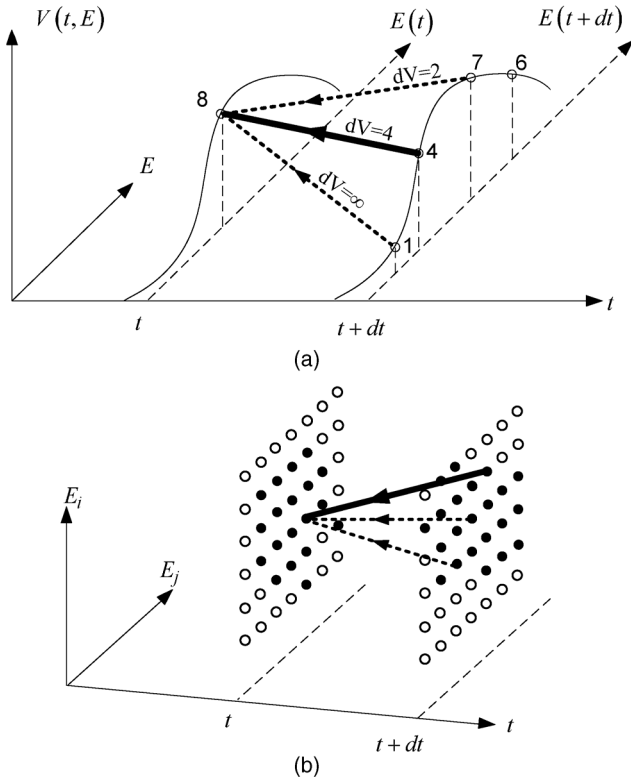


Fig. 4. Backward recursion process, using the Bellman equation. The value function at each point equals the minimum over all differential paths from t to $t + dt$. Possible paths appear as dashed lines, and the optimal path is marked bold. (a) Single storage device, with one state variable $E(t)$. (b) Multidimensional—two storage devices with two variables— $E_i(t)$, $E_j(t)$. White dots mark the numerical grid. Black dots mark feasible solutions.

The differential cost ΔV is computed for 2-D points $\{t, E_i(t), E_j(t)\}$ and $\{t + dt, E_i(t + dt), E_j(t + dt)\}$ [see Fig. 4(b)]. The computation involves evaluation of two derivatives as

$$\begin{aligned} \frac{d}{dt}E_i &\approx \frac{E_i(t + dt) - E_i(t)}{dt} \\ \frac{d}{dt}E_j &\approx \frac{E_j(t + dt) - E_j(t)}{dt}. \end{aligned} \quad (15)$$

These are employed for computing the output power of both storage devices. Using this data, the network power flow is evaluated normally, at each time point, using Gauss–Seidel, or Newton–Raphson. The differential ΔV is assigned a value according to the power at the PCC or assigned a value of infinity in case the solution is infeasible.

Three phase storage devices may be 1-D or 3-D. A balanced three-phase device, with equal powers $P_{i,A} = P_{i,B} = P_{i,C}$, is 1-D. The stored energy $E(t)$ determines the three phase powers, in accordance with the storage state equation (4). Knowing the storage output powers, a three-phase power flow analysis is computed at each time point. If phase powers are each individually controlled, using a dedicated power converter, than the problem is 3-D. The free variables may be $P_{i,A}(t), P_{i,B}(t), P_{i,C}(t)$.

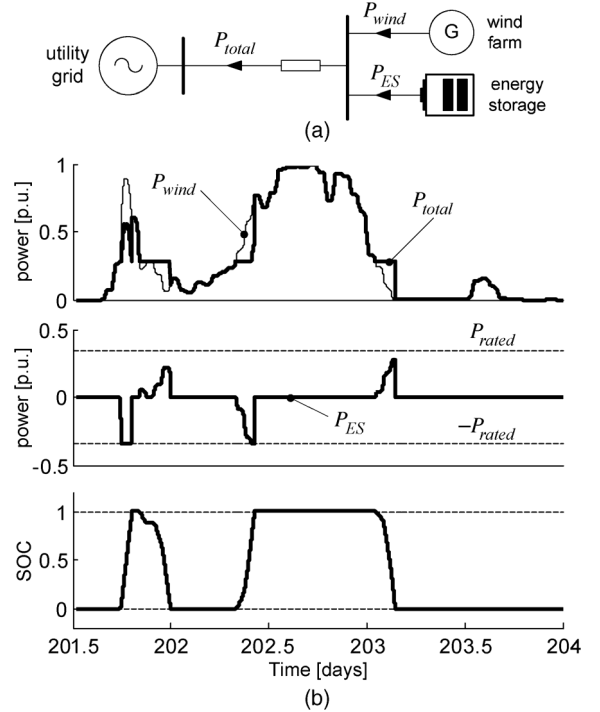


Fig. 5. Power system of Brekken *et al.* [16]. (a) Wind farm and storage. (b) Optimal solution. Top: wind power and total power. Middle: storage power. Bottom: battery SOC.

V. MICROGRID CASE STUDY I

To demonstrate the proposed method, we examine a power system proposed by Brekken *et al.* [16]. The system [Fig. 5(a)] includes a wind farm (renewable source), coupled with a battery energy storage. During high winds, energy is stored in the battery. Stored energy is released when wind is low, smoothing total power injected to the grid.

The following description is duplicated from [16]: wind power is represented by P_{wind} , storage power is P_{ES} , and total power is P_{total} . The battery is modeled by its power capacity P_{rated} , the storage capacity J_{rated} , and the battery State of Charge (SOC), in the range $0 \dots 1$. This represents energy in this problem. The storage state equations are

$$\begin{aligned} \frac{d}{dt}SOC &= -\frac{\eta \cdot P_{ES}}{J_{rated}} \\ \eta &= \begin{cases} \eta_{out}, & P_{ES} > 0 \\ \eta_{in}, & P_{ES} < 0 \end{cases} \\ -P_{rated} &\leq P_{ES} \leq P_{rated} \\ 0 &\leq SOC \leq 1. \end{aligned} \quad (16)$$

The parameters are chosen as follows: $P_{rated} = 0.34$, $J_{rated} = 0.4$, $\eta_{in} = 0.85$, and $\eta_{out} = 1.15$. Wind power P_{wind} is sampled from [16].

The proposed dynamic programming analysis is applied to this system, optimizing the utilization of storage. A price signal is unavailable, so a minimal price objective cannot be evaluated. Instead, we chose to optimize the power output of the system by minimizing losses over the mutual power line. Assuming a

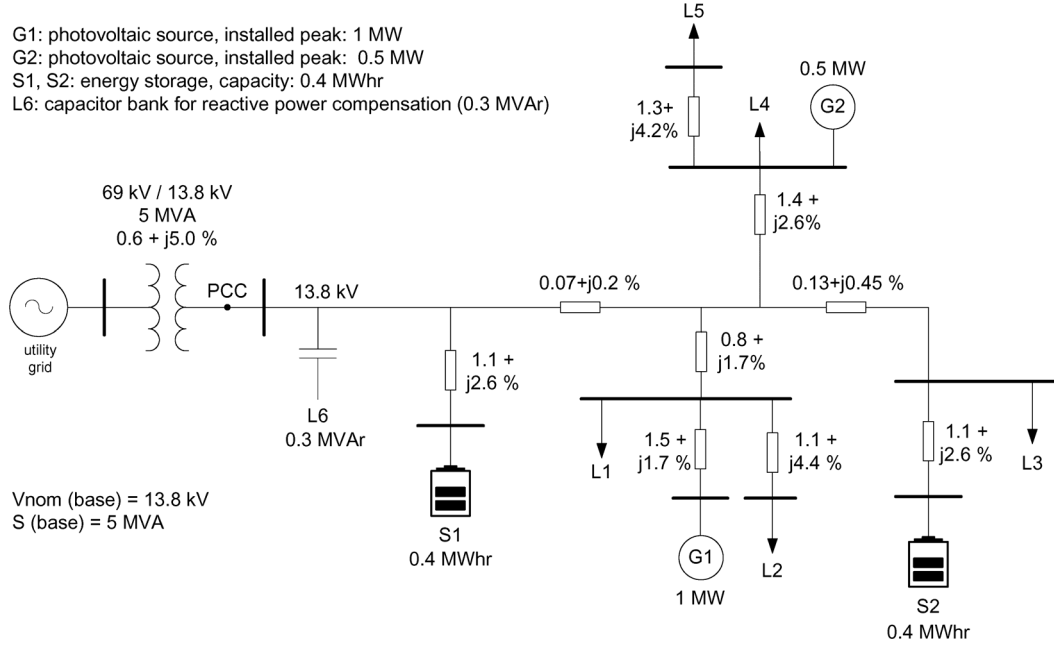


Fig. 6. Microgrid case study II.

resistance of $R = 0.01$ and a bus voltage $V_1 = 1.0$, the objective is

$$\int_0^T \left(P_{\text{total}} - \frac{R}{V_1^2} \cdot P_{\text{total}}^2 \right) dt \rightarrow \min. \quad (17)$$

The value function $V(\cdot)$ is defined over time and the state of charge SOC. It embeds the objective as follows:

$$V(t, \text{SOC}) = \int_t^T \left(P_{\text{total}}(\tau) - \frac{R}{V_1^2} \cdot P_{\text{total}}^2(\tau) \right) d\tau \quad (18)$$

with an initial condition $\text{SOC}(t) = \text{SOC}$

The analysis is computed over a numeric grid, using time step of $dt = 0.1$ h, and $dE = d(\text{SOC}) = 0.01$. $V(\cdot)$ is evaluated using backward recursion, scanning all possible paths of SOC over time. Then, the optimal function $\text{SOC}(t)$ is constructed by forward recursion. Optimal power flow results are shown in Fig. 5(b).

VI. MICROGRID CASE STUDY II

The second system case study combines both a nontrivial network and storage devices. Power flow is optimized to satisfy both the storage device constraints and the physical constraints of the network. The objective is to optimize the cumulative price of energy at the PCC [(5)].

The network is shown at Fig. 6. This microgrid is a medium-voltage (MV) network. It is supplied by a central transformer at the PCC, which ratings are: $V_1(t) = V_{\text{in}}(t) = 13.8$ kV, $S_{\text{nom}} = 5$ MVA. Impedances are specified in per-unit (in percent), using a base equal to the transformer's ratings. Active

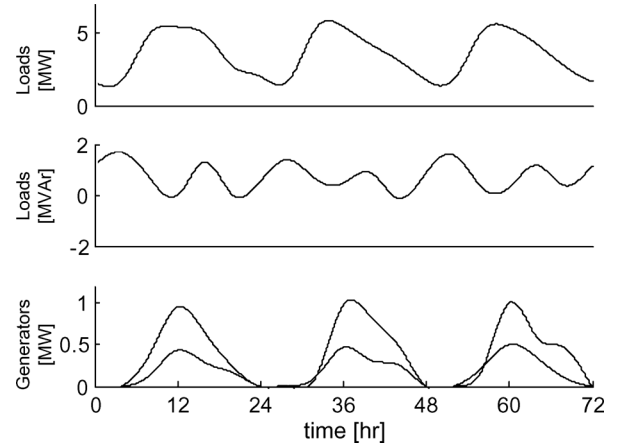


Fig. 7. Microgrid case study II. Powers of loads and generators. Top: sum of active load power. Middle: sum of reactive load power. Bottom: active power of generators.

power at the PCC is limited by the transformer: $-5 \leq P_1(t) \leq +5$ MW.

The microgrid contains two renewable generators, six loads (the sixth is a capacitor bank), and two storage devices. The generators are photovoltaic sources having installed power peaks of 1 and 0.5 MW. They provide only active power. Power signals were generated randomly, over a 72-h period, as shown in Fig. 7. The storage device capacities are $E_{\text{max}} = 0.4$ MWhr each. The storage state equation is

$$\begin{aligned}
 \frac{d}{dt} E_i &= -\alpha \cdot E_i - \mu(P_i) \cdot P_i \\
 \mu(P_i) &= \begin{cases} \frac{1}{\eta_0}, & P_i \geq 0 \\ \eta_0, & P_i < 0 \end{cases} \\
 0 &\leq E_i(t) \leq E_{i,\text{max}}
 \end{aligned} \quad (19)$$

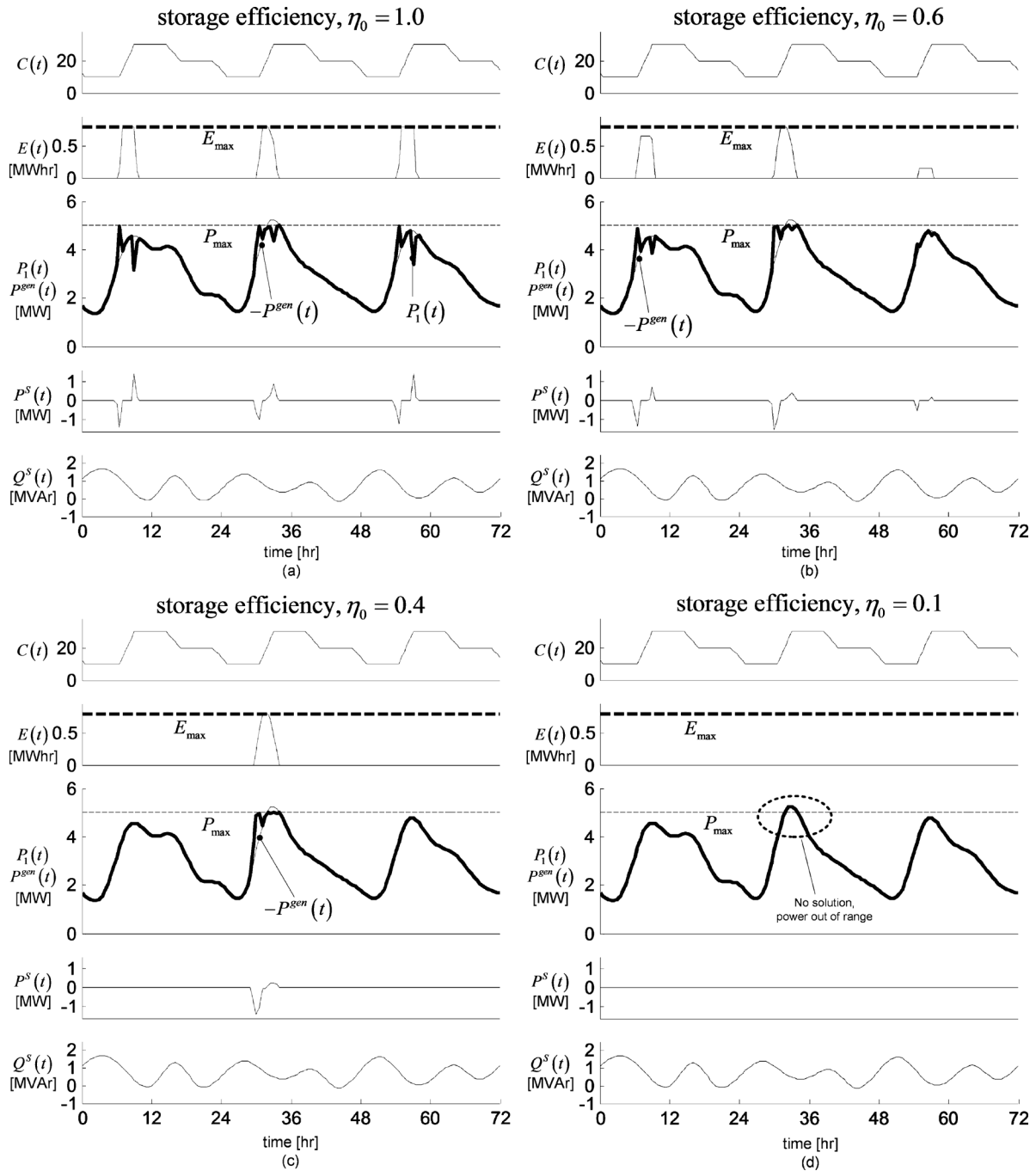


Fig. 8. Microgrid case study II. Resulting optimal powers for different values of storage efficiency. (a) $\eta_0 = 1.0$. (b) $\eta_0 = 0.6$. (c) $\eta_0 = 0.4$. (d) $\eta_0 = 0.1$. The graphs from top to bottom: $C(t)$ —price. $E(t)$ —stored energy. $P_1(t)$ is the power supplied by the utility grid (at the PCC), $P^{gen}(t)$ —the combined active power generation of all loads and renewable generators (taken negative). $P^S(t)$ —combined active power supplied by the storage devices. $Q^S(t)$ —combined reactive power supplied by the storage devices.

where $E_{i,max}$ is the capacity of the device, α is the rate of self-discharge, and η_0 is the efficiency of the device. The chosen parameters are: $E_{i,max} = 0.4$ MWhr for each device, and $\alpha = 0.021/h$. η_0 is varying, taking the values of $\eta_0 = 1.0, 0.6, 0.4$, and 0.1 .

Power flow is optimized using a 1-D process (Fig. 4). The two storage devices have the same ratings and are treated as a unified device. $V(t, E)$ is numerically computed by backward recursion [(8)–(11)], with $dt = 0.5$ h, $dE = 0.05$ MWh. At each time step, network power flow is solved using the simple

Gauss–Seidel analysis. Optimal stored energy is rebuilt by forward recursion [(12)]. The resulting optimal power signals are shown in Fig. 8.

VII. DISCUSSION

This work proposes an optimal power flow analysis, integrating storage devices. An exact global solution to this problem has not been shown so far, due to the numerical complexity of the problem, which includes both the network and time domains, related with storage. Traditional solvers view the

problem as a function to be minimized. This way of thinking leads to traditional solution methods, such as gradient search and linear programming. However, traditional solvers, such as Newton–Raphson, are inefficient in the time domain (see Section III). We propose a new way of thinking, which leads to an entirely different solution, capable of circumventing the numerical complexity: Instead of looking at the problem as a function to be minimized within constraints, we regard stored energy as a resource to be allocated. Instead of a *minimization* problem, we view it as an *allocation* problem: energy is allocated in the time domain to optimize power import at the PCC.

Allocation problems are easily solved by dynamic programming algorithms, so this is the main “engine” of our solver. The solver combines a recursive dynamic programming scan on time domain, with a traditional solver (we used Gauss–Seidel) on the network domain. The solution process is general, and can be used with any network topology (single-phase, balanced, or unbalanced three-phase). Likewise, there is no assumption on the power-flow solver, which can be Newton–Raphson, Gauss–Seidel, or a specific per-phase solver, such as forward backward sweep or TCIM. At each time point, the value function $V(\cdot)$ is evaluated in respect to a previous value. The network power flow is solved at each time point, after replacing the storage devices with dummy P – V sources. This power output is evaluated only by the current and previous energy values. Thus, each time point is evaluated once. There is no need to recompute the entire energy path, so the calculation is numerically efficient.

The dynamic programming approach presents several important advantages: First, it reveals the globally optimal solution, since the algorithm scans the entire solution space. Second, the model is extremely general. It does not bind to a certain model or constraint. Storage device are described by general state equations [(3) and (4)]. Different storage devices with entirely different properties may be integrated in the same network. One-phase networks may be solved just as well as three-phase networks. Different objective functions may be considered [(5)–(7) and (17)]. The solution method is always the same: a recursive scan of all feasible system states.

A main disadvantage of the propose approach is that numerical complexity grows in power law with the number of (different) storage devices. This is evident in Fig. 4(b): each storage device contributes an extra dimension to the solution space. From our experience, a network with a single storage device is evaluated in seconds, even if it contains hundreds of buses. However, a system with four or five devices may be evaluated if it contains only a few buses.

Two system case studies are shown. The first system is a two bus topology (Fig. 5). The second system (Fig. 6) is a network, with two renewable sources and two storage devices. The systems differ in both topology and design objectives and employ different storage devices. The objective in the first system is to minimize loss over the transmission line, whereas, in the second system, the objective is to minimize the price of imported energy. The same dynamic programming analysis is applied to both systems. The cost function $V(\cdot)$, shown in (8), is defined, and evaluated by backward-recursion, as shown in (9)–(11). Optimal stored energy and power flow is revealed by forward recursion, described in (12).

The resulting optimal power management (Figs. 5 and 8) reveals a similar conceptual strategy for both systems: energy is stored according to the availability of the primary source: wind power, in the first example, or low-cost energy at the PCC, in the second example. Stored energy is released to the network when wind power is not available (first example) or when the price of energy is too high (second example). In both systems, stored energy tends to equalize the total power, in order to reduce losses as much as possible. The second system includes the nonzero admittances of power lines, and the power limit of the transformer. This topology of the network effects the management of stored energy. For example, the storage device compensates the load, to sustain the 5-MVA capacity of the PCC’s transformer, as shown in Fig. 8(c). Fig. 8 reflects the effect of storage efficiency (η_0) on power management. In Fig. 8(a), ($\eta_0 = 1$), the storage is charged to full capacity. In Fig. 8(b), ($\eta_0 = 0.6$), losses are higher, and the storage is not fully charged. In Fig. 8(c), ($\eta_0 = 0.4$), the storage device is so lossy that it becomes economically worthless. In Fig. 8(d), ($\eta_0 = 0.1$), the storage losses dominates. Here, the storage device cannot supply enough power to compensate the load’s power peak, and the network will become unstable. There is no feasible solution.

VIII. CONCLUSION

This work suggests an algorithm to compute the optimal energy management of storage devices in grid-connected microgrids. Stored energy is controlled to balance the power of loads and renewable sources, over the time domain, minimizing the overall cost of energy at the PCC. The algorithm incorporates an arbitrary network topology, which can be a general one-phase, balanced, or unbalanced three-phase system. It employs a power flow solver in network domain, within a dynamic programming recursive search in time domain. This combination is robust and numerically efficient and reveals the globally optimal stored energy versus time for each storage device.

REFERENCES

- [1] J. C. Vasquez, J. M. Guerrero, J. Miret, M. Castilla, and L. G. de Vicuña, “Hierarchical control of intelligent microgrids,” *IEEE Ind. Electron. Mag.*, vol. 4, pp. 23–29, Dec. 2010.
- [2] E. Barklund, N. Pogaku, M. Prodanovic, C. Hernandez-Aramburo, and T. C. Green, “Energy management in autonomous microgrid using stability-constrained droop control of inverters,” *IEEE Trans. Power Electron.*, vol. 23, no. 9, pp. 2346–2352, Sep. 2008.
- [3] J. Arai, K. Iba, T. Funabashi, Y. Nakanishi, K. Koyanagi, and R. Yokoyama, “Power electronics and its applications to renewable energy in Japan,” *IEEE Circuits Syst. Mag.*, vol. 8, pp. 52–66, 2008.
- [4] F. Katiraei, R. Iravani, N. Hatziargyriou, and A. Dimeas, “Microgrids management,” *IEEE Power Energy Mag.*, vol. 6, pp. 54–65, May–Jun., 2008.
- [5] R. H. Lasseter, “Microgrids,” in *Proc. IEEE Power Eng. Soc. Winter Meeting*, Feb. 2001, vol. 1, pp. 146–149.
- [6] A. G. Tsikalakis and N. D. Hatziargyriou, “Centralized control for optimizing microgrids operation,” *IEEE Trans. Energy Conv.*, vol. 23, no. 2, pp. 241–248, Mar. 2008.
- [7] R. Majumder, A. Ghosh, G. Ledwich, and F. Zare, “Power management and power flow control with back-to-back converters in a utility connected microgrid,” *IEEE Trans. Power Syst.*, vol. 25, pp. 821–834, May 2010.
- [8] V. Del Toro, *Electric Power Systems*. Englewood Cliffs, NJ, USA: Prentice-Hall, 1992, vol. II.
- [9] N. P. Padhy, “Unit commitment—A bibliographical survey,” *IEEE Trans. Power Syst.*, vol. 19, no. 2, pp. 1196–1205, May 2004.

- [10] Y. Atwa, E. El-Saadany, M. Salama, and R. Seethapathy, "Optimal renewable resources mix for distribution system energy loss minimization," *IEEE Trans. Power Syst.*, vol. 25, no. 1, pp. 360–370, Feb. 2010.
- [11] H. Nikkhajoei and R. Iravani, "Steady-state model and power flow analysis of electronically-coupled distributed resource units," *IEEE Trans. Power Del.*, vol. 22, no. 1, pp. 721–728, Jan. 2007.
- [12] G. Celli, E. Ghiani, S. Mocci, and F. Pilo, "A multiobjective evolutionary algorithm for the sizing and siting of distributed generation," *IEEE Trans. Power Syst.*, vol. 20, no. 2, pp. 750–757, May 2005.
- [13] Y. Levron and D. Shmilovitz, "Power systems' optimal peak-shaving applying secondary storage," *Electr. Power Syst. Res.*, vol. 89, pp. 80–84, Aug. 8, 2012.
- [14] Y. Levron and D. Shmilovitz, "Optimal Power Management in Fueled Systems With Finite Storage Capacity," *IEEE Trans. Circuits Syst. I, Reg. Papers*, vol. 57, no. 8, pp. 2221–2231, Aug. 2010.
- [15] J. P. Barton and D. G. Infield, "Energy storage and its use with intermittent renewable energy," *IEEE Trans. Energy Conv.*, vol. 19, no. 2, pp. 441–448, Jun. 2004.
- [16] T. K. A. Brekken, A. Yokochi, A. von Jouanne, Z. Z. Yen, H. M. Hapke, and D. A. Halamaj, "Optimal energy storage sizing and control for wind power applications," *IEEE Trans. Sustainable Energy*, vol. 2, no. 1, pp. 69–77, Jan. 2011.
- [17] J. C. M. Vieira, W. Freitas, and A. Morelato, "Phase-decoupled method for three-phase power-flow analysis of unbalanced distribution systems," *Proc. Inst. Electr. Eng.—Gen., Transm. Distrib.*, vol. 151, pp. 568–574, Sept. 2004.
- [18] D. P. Bertsekas, *Dynamic Programming and Optimal Control*. Belmont, MA, USA: Athena Scientific, 1995, vol. 1.



Yoash Levron received the Ph.D. degree from Tel-Aviv University, Tel Aviv, Israel.

His research interests include power electronics, power systems and distributed power management.



Josep M. Guerrero (S'01–M'04–SM'08) received the B.S. degree in telecommunications engineering, M.S. degree in electronics engineering, and Ph.D. degree in power electronics from the Technical University of Catalonia, Barcelona, Spain, in 1997, 2000, and 2003, respectively.

He is a Full Professor with the Institute of Energy Technology, Aalborg University, Aalborg, Denmark, where he is responsible for the Microgrid research program. His research interests include power electronics converters for distributed generation and distributed energy storage systems, control and management of microgrids and islanded minigrids, and photovoltaic and wind power plants control.

Prof. Guerrero is an associate editor of the IEEE TRANSACTIONS ON INDUSTRIAL ELECTRONICS, the *IEEE Industrial Electronics Magazine*, and the IEEE TRANSACTIONS ON POWER ELECTRONICS.



Yuval Beck received the B.Sc., M.Sc., and Ph.D. degrees from Tel-Aviv University, Tel Aviv, Israel, in 1997, 2002, and 2007, respectively, all in electrical engineering.

He is head of the Energy and Power Systems Department, Holon Institute of Technology (HIT), Holon, Israel. His fields of interest are: power systems, power electronics, lightning phenomena, photovoltaic systems, and smart grid.